The Transition State for Carboxylic Acid Deprotonation on Cu(100)

Boonchuan Immaraporn,[†] Pingping Ye,[†] and Andrew J. Gellman*,[‡]

Department of Chemistry and Department of Chemical Engineering, Carnegie Mellon University, Pittsburgh, Pennsylvania 15213

The kinetics of acid deprotonation on the Cu(100) surface have been studied using four different fluorinated carboxylic acids (CF_2HCO_2H, CF_3CO_2H, $CF_2HCF_2CO_2H$, and $CF_3CF_2CO_2H$). All four acids adsorb molecularly on Cu(100) at 90 K but deprotonate during heating to form carboxylates on the surface at temperatures below 300 K. Temperature-programmed reaction spectroscopy and X-ray photoemission spectroscopy were used to verify that the acids deprotonate on the Cu(100) surface. Work function measurements were used to study the deprotonation kinetics during heating and to estimate the activation energy barriers ($\Delta E^{\ddagger}_{O-H}$) to deprotonation. The nature of the transition state to acid deprotonation on Cu(100) was probed by analysis of linear free energy relationships (LFER) or correlations of $\Delta E^{\ddagger}_{O-H}$ with the acid substituent constants, σ_F. The field reaction constant, ρ_F, or the slope of the LFER was found to be $\rho_F = -52 \pm 13$ kJ/mol in the limit of zero coverage and $\rho_F = -19 \pm 2$ kJ/mol at a coverage of 1/2 ML. These values of ρ_F can be compared to the value of $\rho_F = -104$ kJ/mol for acid deprotonation in the gas phase. This comparison suggests that the transition state for acid deprotonation on Cu(100) must be anionic with respect to the reactant ($RCO_2H_{(ad)} \leftrightarrow [RCO_2^{\delta-}\cdots H^{\delta+}]^{\ddagger} \rightarrow$).

1. Introduction

Since heterogeneous catalysis is fundamentally a kinetic phenomenon, characterizing the transition states to elementary steps in catalytic surface reaction mechanisms is critical to understanding the influence of catalysts on activation barriers and catalytic reaction kinetics. Unfortunately, few experimental approaches to examining the nature of transition states on surfaces are available. One approach is to use substituent effects, a method that has often been employed in gas-phase and solution-phase reactions. The application of substituent effects in surface chemistry, however, is still limited.[1] The elimination of β-hydride in alkoxides on the Cu(111) surface is an example of a surface reaction in which substituent effects have been used to show that the transition state is cationic with respect to the reactant, $[RC^{\delta+}\cdots H^{\delta-}]^{\ddagger}$.[2,3] Another reaction for which substituent effects have been used as probes of the transition state is the dehalogenation of alkyl iodides on Ag(111) and Pd(111) surfaces.[4–6] Deiodination kinetics were measured using a series of alkyl iodides with a wide range of substituent groups. In that case the transition state was found to be homolytic or reactant-like, $[RC^{\bullet}\cdots I^{\bullet}]^{\ddagger}$. The use of substituent effects is broadly applicable and can be a valuable tool for expanding the scope of our understanding of catalytic processes.[7–9]

The work presented in this paper expands on a previous study of the nature of the transition state for carboxylic acid deprotonation on Ag single-crystal surfaces.[10] That work examined the surface chemistry of CH_3CO_2H and CF_3CO_2H on Ag(111) and Ag(110) surfaces. In summary, CH_3CO_2H adsorbs reversibly on the Ag surfaces and desorbs during heating while CF_3CO_2H deprotonates on the surface to form CF_3CO_2-Ag. Unfortunately, measurement of the deprotonation kinetics was

complicated by the fact that a fraction of the adsorbed CF_3CO_2H desorbed during heating. Although the barrier to deprotonation, $\Delta E^{\ddagger}_{O-H}$, of CF_3CO_2H was shown to be lower than that of CH_3CO_2H, the results did not allow us to distinguish between heterolytic and homolytic descriptions of the transition state for acid deprotonation on the Ag(111) surface. A more quantitative study requires surfaces on which the deprotonation reaction is substantially faster than desorption. Carboxylic acids are known to deprotonate on single-crystal surfaces of metals such as Cu[11–17] or Pt.[18,19] Since there have been a number of studies of both carboxylic acids and carboxylates on Cu surfaces, they are good candidates for a thorough study of acid deprotonation kinetics.

The surface chemistry of formic acid and acetic acid has been studied on all three low Miller index surfaces of copper. On the Cu(110) surface, Bowker and Madix found that acetic acid adsorbs molecularly on the clean surface at 140 K.[16] During heating, acid deprotonation occurred at temperatures between 140 and 375 K to produce adsorbed formate and acetate. Molecular desorption of acetic acid was also observed at 240 K. The hydrogen atoms generated on the surface as a result of deprotonation recombine to desorb as H_2 at 310 K. The formate and acetate were stable during heating until the temperature reached ∼600 K, at which point they decomposed to produced H_2, CO_2, and other species that desorbed into the gas phase. The barrier to the deprotonation of acetic acid on the Cu(110) surface was measured by Lee et al. and found to vary from $\Delta E^{\ddagger}_{O-H} = 37.6$ kJ/mol at low coverages to $\Delta E^{\ddagger}_{O-H} = 106$ kJ/mol at high coverages.[11] The focus of the work described in this paper is the nature of the transition state to deprotonation of acids on the Cu(100) surface which will be probed through measurements of $\Delta E^{\ddagger}_{O-H}$. Clearly, the existing studies indicate that attention must be paid to the coverage dependence of these measurements.

We have attempted to probe the nature of the transition state for acid deprotonation on the Cu(100) surface using substituent

---

* Author to whom correspondence should be addressed. E-mail: gellman@cmu.edu.
† Department of Chemistry.
‡ Department of Chemical Engineering.

Carboxylic Acid Deprotonation on Cu(100)

J. Phys. Chem. B, Vol. 108, No. 11, 2004 **3505**

effects. Measurements have been made of the deprotonation reaction kinetics using a series of fluorinated carboxylic acids (CF_2HCO_2H, CF_3CO_2H, $CF_2HCF_2CO_2H$, and $CF_3CF_2CO_2H$) adsorbed on the Cu(100) surface. Temperature-programmed reaction spectroscopy (TPRS) and X-ray photoemission spectroscopy (XPS) were used to show that all four carboxylic acids deprotonate to form carboxylates on the Cu(100) surface at temperatures in the range 150−300 K. The carboxylates decompose during further heating to yield CO_2 and other fluorinated species at temperatures of 500−600 K. TPRS and XPS results show that desorption from the Cu(100) surface is much slower than deprotonation so acid desorption is not detected under any experimental conditions reported in this study. Work function measurements have been used to measure the deprotonation kinetics and thus estimate the barriers to deprotonation, $\Delta E^{\ddagger}_{O-H}$. Correlation of acid substituent constants, σ_F, with the $\Delta E^{\ddagger}_{O-H}$ shows that the transition state for acid deprotonation on Cu(100) is anionic with respect to the adsorbed acid ($RCO_2H_{(ad)} \leftrightarrow [RCO_2^{\delta-}\cdots H^{\delta+}]^{\ddagger} \rightarrow$).

2. Experimental Section

All experiments were performed in an UHV chamber equipped with an Ar^+ ion gun for cleaning the Cu(100) crystal surface, leak valves for gas dosing, an Al Kα X-ray source and VG CLAM II hemispherical analyzer for X-ray photoelectron spectroscopy (XPS), and a Dycor quadrupole mass spectrometer for desorption measurements. The Cu(100) single-crystal sample was mounted by spot-welding between two Ta wires on a small sample holder which was then bolted to the end of the UHV sample manipulator. The manipulator allows cooling of the samples to $T < 100$ K and resistive heating to $T > 1000$ K. A chromel−alumel thermocouple was spot-welded to the edge of the Cu sample for temperature measurement.

The Cu(100) sample was purchased from Monocrystals Inc. and was cleaned by several cycles of Ar^+ ion sputtering followed by annealing to 1000 K. XPS was used to monitor the cleanliness of the Cu(100) surface.

The experiments used several fluorocarbon carboxylic acids (CF_2HCO_2H, CF_3CO_2H, $CF_2HCF_2CO_2H$, and $CF_3CF_2CO_2H$) obtained from Aldrich Chemical Co. The acids are all liquids at room temperature and were purified by several cycles of freeze−pump−thawing. The purity of the vapor introduced into the UHV chamber through the leak valves was verified by mass spectrometry. The acids were adsorbed on the clean Cu(100) surfaces at 90 K by backfilling the chamber through a leak valve.

Temperature-programmed reaction spectroscopy (TPRS) was performed using the Dycor mass spectrometer to monitor the desorption signals at several m/q ratios simultaneously while the sample was heated at a rate of 2 K/s. X-ray photoelectron spectroscopy (Al Kα X-ray source and a VG CLAM II hemispherical analyzer) was performed with an X-ray source power of 600 W and an analyzer pass energy of 30 eV. The scan times were approximately 15 minutes for the C 1s and O 1s spectra, and 5 minutes for the F 1s spectra. The binding energies of the XPS peaks were calibrated assuming that the values for the Cu peaks were Cu $3p_{3/2} = 75$ eV, Cu $3p_{1/2} = 77$ eV, Cu $3s = 123$ eV, Cu $2p_{3/2} = 933$ eV, Cu $2p_{1/2} = 953$ eV, and Cu $2s = 1097$.[20] The surface work function was measured using a Kelvin probe (Besocke Delta PHI GmbH) with the sample positioned approximately 1 mm from the vibrating gold mesh electrode during heating. The work function was measured with a heating rate of 0.2 K/s and a time constant of $t_c = 3$ s.

TPRS of CF_2HCO_2H / Cu(100)
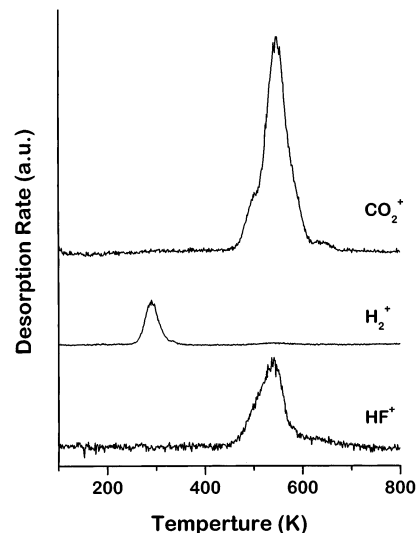
Figure 1. TPR spectrum of CF_2HCO_2H monolayer on the Cu(100) surface at saturation coverage. The heating rate was $\beta = 2$ K/s. Signals were monitored at $m/q = 2$, 20, and 44.

3. Results

3.1. CF_2HCO_2H on Cu(100). The CF_2HCO_2H monolayer is irreversibly adsorbed on the Cu(100) surface and decomposes during heating. TPRS of a CF_2HCO_2H monolayer on Cu(100) is shown in Figure 1. The monolayer is defined as the highest coverage that can be adsorbed on the Cu(100) surface before some multilayer desorption is observed during TPRS measurements. H_2, HF, and CO_2 desorption signals at $m/q = 2$, 20, and 44 amu were monitored during heating. H_2 desorption is detected at $T \sim 300$ K while CO_2 and HF desorption occur at $T \sim 540$ K. The TPR spectra of CF_2HCO_2H suggest that during heating the acid deprotonates to form CF_2HCO_2 on the surface at temperatures below 300 K. At 290 K the H atoms recombine and desorb from the surface as a H_2. Desorption of H_2 at this temperature is rate limited by H atom recombination.[21] CF_2HCO_2 is stable on the surface at temperatures up to $T \sim 450$ K at which point it begins to decompose to yield desorption of CO_2, HF, and other fragments.

XPS has been used to show that the CF_2HCO_2H decomposition intermediate is CF_2HCO_2. Figure 2 shows C 1s and O 1s XP spectra of the CF_2HCO_2H monolayer adsorbed on the Cu(100) surface at 90 K. The C 1s spectrum of the CF_2HCO_2H monolayer exhibits a major peak at a binding energy of 289.4 eV with a small shoulder at 288.2 eV. After annealing to 350 K, the C 1s region reveals two poorly resolved peaks at 287.2 and 288.5 eV which have similar intensity and are assigned to the $-CO_2$ and $-CF_2H$ groups of CF_2HCO_2, respectively. The O 1s XP peak in CF_2HCO_2H adsorbed at 90 K is observed at a binding energy of 531.8 eV with a peak width of ~2.5 eV. After annealing the Cu(100) surface to 350 K, the O 1s peak shifts from 531.8 to 530.6 eV and the peak width decreases from 2.5 to 1.8 eV. The C 1s and O 1s peak shifts are consistent with a reaction mechanism in which CF_2HCO_2H adsorbs molecularly onto the Cu(100) surface at 90 K and then undergoes deprotonation to form CF_2HCO_2 on the surface upon annealing to 350 K. The proposed formation of CF_2HCO_2 is supported by the decrease in the O 1s XP peak width upon heating the surface to 350 K, indicating that both oxygen atoms become chemically equivalent in their bonding to the Cu(100)

C 1s and O 1s XPS - CF$_2$HCO$_2$H / Cu(100)
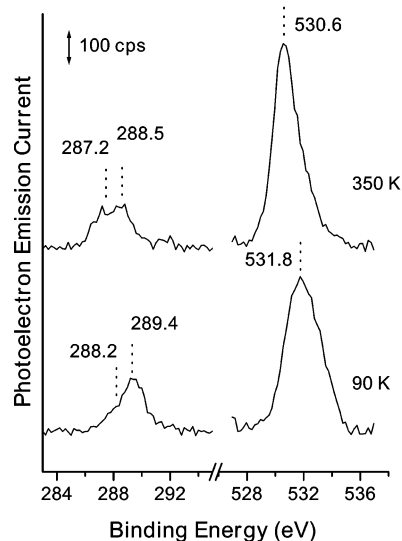
Figure 2. C 1s and O1s XP spectra of CF$_2$HCO$_2$H on the Cu(100) surface at 90 K and after annealing the surface to 350 K. After heating to 350 K, the C 1s photoemission peaks from the −CO$_2$ and CF$_2$H− groups appear at 287.2 and 288.5 eV, respectively. The O1s spectrum for CF$_2$HCO$_2$H obtained at 90 K reveals a broad peak at a binding energy of 531.8 eV. After heating the surface to 350 K to produce the adsorbed CF$_2$HCO$_2$, the O 1s peak shifts to 530.6 eV and becomes significantly narrower.

TPRS of CF$_2$HCF$_2$CO$_2$H / Cu(100)
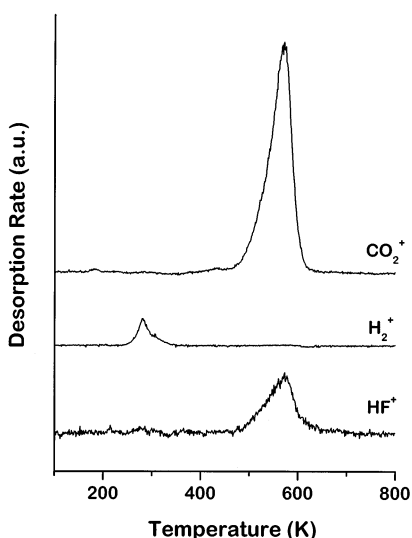
Figure 3. TPR spectrum of the CF$_2$HCF$_2$CO$_2$H monolayer on the Cu(100) surface at saturation coverage. The heating rate was $\beta = 2$ K/s. Signals were monitored at m/q = 2, 20, and 44.

surface. The decrease in the binding energy is consistent with the formation of an anionic −CO$_2$ group.

3.2. CF$_2$HCF$_2$CO$_2$H on Cu(100). As in the case of CF$_2$-HCO$_2$H, TPR spectra (Figure 3) indicate that CF$_2$HCF$_2$CO$_2$H deprotonates on the Cu(100) surface at temperatures below 300 K. During heating, H$_2$ desorption is observed at 280 K in the TPR spectra. CF$_2$HCF$_2$CO$_2$, the deprotonation product, remains stable on the surface up to temperatures of ∼500 K, at which point it begins to decompose to yield HF and CO$_2$ desorption. Note that molecular desorption does not appear in the TPR spectra, indicating that all of the adsorbed acid deprotonates on the Cu(100) surface.

C 1s and O 1s XPS - CF$_2$HCF$_2$CO$_2$H / Cu(100)

Figure 4. C 1s and O1s XP spectra of CF$_2$HCF$_2$CO$_2$H on the Cu(100) surface at 90 K and after annealing the surface to 350 K. After heating to 350 K, the C 1s photoemission peaks from the −CO$_2$, and CF$_2$-HCF$_2$− groups appear at 288.0 and 289.3 eV, respectively. The O 1s spectrum of CF$_2$HCF$_2$CO$_2$H obtained at 90 K reveals one broad peak at a binding energy of 532.5 eV. After heating the surface to 350 K to produce the adsorbed CF$_2$HCF$_2$CO$_2$, the O 1s peak shifts to 531 eV and becomes significantly narrower.

XP spectra of CF$_2$HCF$_2$CO$_2$H on the Cu(100) surface are also consistent with a process in which the acid adsorbs molecularly at 90 K and then deprotonates during heating. The C 1s peak shown in Figure 4 for the molecular species is centered at 290.3 eV and is broad as a result of the contributions from the −CO$_2$H, −CF$_2$H, and −CF$_2$− groups. The O 1s feature is centered at 532.5 eV and is quite broad due to the contributions from two inequivalent oxygen atoms. Upon annealing the surface to 350 K, the C 1s peaks shift to 289.3 and 288 eV and the O 1s peak shifts from 532.5 to 531 eV. The C 1s peaks have a 2:1 intensity ratio consistent with assignment to the −CF$_2$− and −CF$_2$H groups and to the −CO$_2$ group. The O1s peak width also decreases as the surface is annealed from 90 to 350 K, consistent with the formation of a CF$_2$HCF$_2$CO$_2$ species with two equivalent oxygen atoms.

3.3. CF$_3$CO$_2$H and CF$_3$CF$_2$CO$_2$H on Cu(100). TPRS and XPS studies of CF$_3$CO$_2$H and CF$_3$CF$_2$CO$_2$H on the Cu(100) surface have yielded results that are similar to those described above for CF$_2$HCF$_2$CO$_2$H and CF$_2$HCO$_2$H. They reveal deprotonation of both acids to yield the corresponding carboxylates on the Cu(100) surface at temperatures below 300 K. During heating, the adsorbed hydrogen atoms generated by deprotonation recombine at ∼300 K to desorb as H$_2$. The carboxylates then remained as stable intermediates on the Cu(100) surface up to temperatures of >450 K, at which point they begin to decompose. Products of the decomposition reactions that decompose into the gas phase include CO$_2$, HF, CF$_3$, and other fluorinated species. Decreases in the O 1s binding energy by 1.3−1.5 eV are observed as the surface temperature increases from 90 to 350 K. In addition, the O 1s XP peak becomes narrower as the deprotonation of the acid to produce the carboxylate renders both oxygen atoms equivalent. In summary, TPD and XPS studies of all four acids indicate that they adsorb molecularly at 90 K and deprotonate on heating the Cu(100) surface to 300 K. There is no molecular desorption of the acid monolayers.

Carboxylic Acid Deprotonation on Cu(100)

J. Phys. Chem. B, Vol. 108, No. 11, 2004 **3507**

ΔΦ vs. T - CF₂HCO₂H / Cu(100)
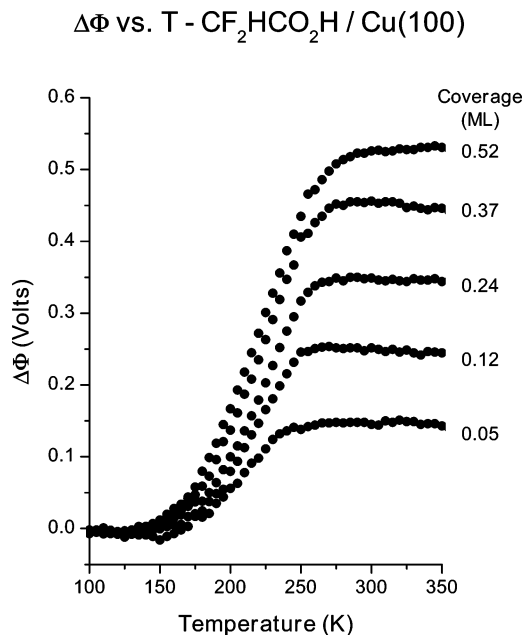
Figure 5. Work function change versus temperature during heating of CF_2HCO_2H on Cu(100) at various initial CF_2HCO_2H coverages. The work function change occurs as a results of the deprotonation of the CF_2HCO_2H to yield adsorbed CF_2HCO_2. The heating rate was $\beta = 0.2$ K/s.

3.4. Acid Deprotonation Kinetics on Cu(100). The deprotonation kinetics of the four acids on the Cu(100) surface have been measured using temperature-programmed work function measurements. The work function changes versus temperature for CF_2HCO_2H adsorbed on Cu(100) at various coverages are displayed in Figure 5. As expected, the deprotonation of the acid leads to large, easily measured changes in the surface work function. The CF_2HCO_2H coverage has been determined from the area under the CO_2 TPR spectrum relative to the amount of CO_2 generated by decomposition of the saturated monolayer. CO_2 desorption has in turn been calibrated using XPS to show that the amount of CO_2 desorption during carboxylate decomposition is in fact linear in the initial carboxylate coverage. For all initial coverages, the spectra in Figure 5 show that the work function remains fairly constant as the surface temperature increases from 90 to 150 K. The work function changes rapidly between 150 and 250 K, but then remains constant until the temperature reaches 350 K. The increase of the work function during heating serves as a measure of the acid deprotonation kinetics on the Cu(100) surface. The magnitude of the work function change ($\Delta\Phi$) also increases as the initial CF_2HCO_2H coverage increases. The $\Delta\Phi$ versus T spectra agree with the mechanism for the surface chemistry proposed on the basis of the TPR and XP spectra. The acid adsorbs molecularly on the surface at 90 K and then deprotonates during heating. The positive change in the work function is consistent with the formation of an anionic carboxylate, $CF_2HCO_2^{\delta-}$, as the product and thus an increase in the surface dipole contribution to the work function. The deprotonation is complete by 250 K, indicating that the desorption of H_2 into the gas phase at 290 K is rate limited by H atom recombination on the Cu(100) surface.[21] Apparently, H atom recombination and desorption as H_2 has very little influence on the work function of the surface.

Measurement of the CF_2HCO_2H deprotonation kinetics requires that we know the extent of reaction or the carboxylate coverage as a function of temperature, $\theta(T)$, during heating. To obtain the $\theta(T)$ relationship from the measured $\Delta\Phi(T)$ curves,

Coverage vs. ΔΦ - CF₂HCO₂H / Cu(100)
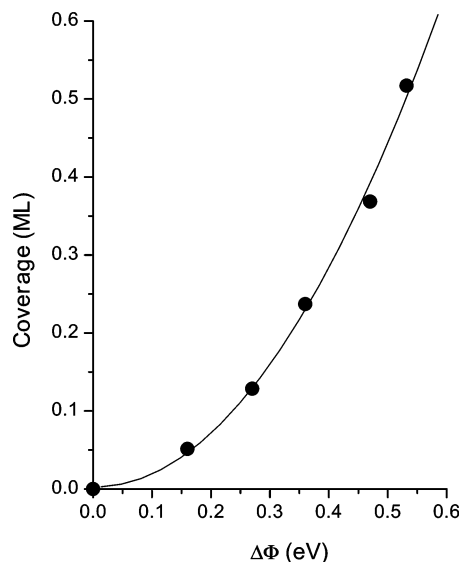
Figure 6. The CF_2HCO_2H coverage versus total work function change ($\Delta\Phi$). The solid line is a fit of a second-order polynomial to the data.

the relationship between the initial CF_2HCO_2H coverage and the work function change, $\theta(\Delta\Phi)$, must be established. This is needed to calibrate the measurement to eliminate any effects that might lead to a nonlinear change of $\Delta\Phi$ with coverage. Figure 6 shows the plot of the initial CF_2HCO_2H coverage on the surface versus the work function change. The initial coverage of the CF_2HCO_2H was determined using the amount of CO_2 desorption observed during thermal decomposition of the CF_2HCO_2 deprotonation product. The $\theta(\Delta\Phi)$ data have been fitted to a second-order polynomial function as shown in Figure 6. The $\Delta\Phi(T)$ spectra shown in Figure 5 can then be transformed into the $\theta(T)$ curves via the fitting polynomial. The coverage of CF_2HCO_2 versus the surface temperature, $\theta(T)$, is displayed in Figure 7 for increasing initial CF_2HCO_2H coverages. The peak temperature, T_p, for the deprotonation reaction is estimated from the temperatures of the inflection points of the curves in Figure 7. These inflection points can be found from the maximum in the $d\theta/dT$ curves shown in Figure 8. These $d\theta/dT$ curves are analogous to the desorption curves observed in TPD spectra and can be used to estimate the value of $\Delta E_{O-H}^{\ddagger}$.

The activation barrier to acid deprotonation, $\Delta E_{O-H}^{\ddagger}$, can be determined from the peak reaction temperature, T_p, using Redhead's equation and assuming first-order kinetics.[22] First, however, one needs to determine the preexponential factor, v, of the deprotonation reaction. To obtain the preexponential factor, work function measurements of $CF_2HCF_2CO_2H$ deprotonation were performed at various heating rates in the range $\beta = 0.05$ to 1 K/s and at various coverages. For each of the heating rates, the value of T_p was determined in the limit of zero coverage. In the zero coverage limit the value of $\Delta E_{O-H}^{\ddagger}$ for $CF_2HCF_2CO_2H$ deprotonation was determined from the slope of $\ln(\beta/T_p^2)$ versus $1/T_p$ shown in Figure 9. The preexponential factor, v, was then calculated using Redhead's equation and the value of $\Delta E_{O-H}^{\ddagger}$. The kinetic parameters for $CF_2HCF_2CO_2H$ deprotonation are $\Delta E_{O-H}^{\ddagger} = 76.6 \pm 3.8$ kJ/mol and $v = 6.2 \times 10^{17}$ s^{-1} in the limit of low coverage. The values of $\Delta E_{O-H}^{\ddagger}$ for deprotonation of all four acids at all coverages studied in this work were then calculated from Redhead's equation using a value of $v = 6.2 \times 10^{17}$ s^{-1} for the preexponential factor and the experimentally determined values of T_p.

CF$_2$HCO$_2$ Coverage vs. Temperature
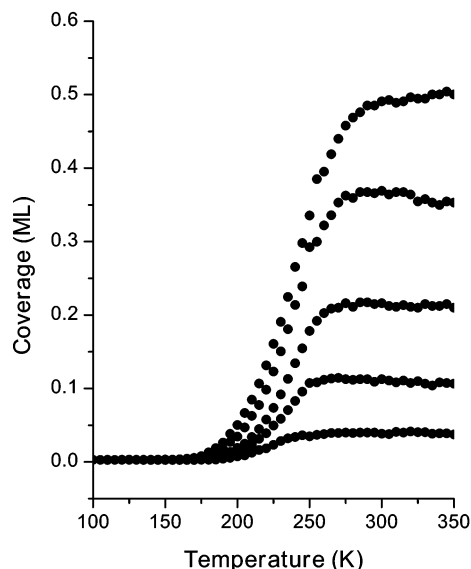
Figure 7. The CF$_2$HCO$_2$ coverage (θ) on the Cu(100) surface versus temperature during heating. The coverage increases as a results of the deprotonation of the adsorbed CF$_2$HCO$_2$H. Curves are plotted for various different initial coverages of the CF$_2$HCO$_2$H. The curves displayed were obtained by converting the work function spectra shown in Figure 5 to the CF$_2$HCO$_2$ coverage by application of the second-order polynomial found in Figure 6.

d θ/*d* T - CF$_2$HCO$_2$H / Cu(100)
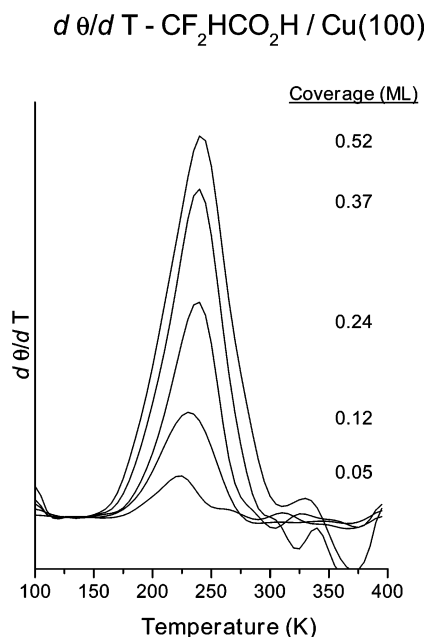
Figure 8. Derivative of the CF$_2$HCO$_2$ coverage with respect to temperature dθ/dT versus surface temperature at various initial CF$_2$HCO$_2$H coverages on the Cu(100) surface. dθ/dT is proportional to the rate of CF$_2$HCO$_2$H deprotonation or CF$_2$HCO$_2$ appearance. These are analogous to desorption spectra.

The work function changes during heating of CF$_3$CO$_2$H, CF$_2$HCF$_2$CO$_2$H, C$_2$F$_5$CO$_2$H adsorbed on the Cu(100) surface display similar trends to that found for CF$_2$HCO$_2$H. The work function is constant for temperatures below 150 K, increases rapidly as the temperature increases from 150 to 300 K, and then levels off once the temperature is increased past 300 K. The $\theta(T)$ curves for all four acids at a coverage of $\theta \approx 0.1$ ML are shown together in Figure 10 for the purpose of comparison. The

Deprotonation - CF$_2$HCF$_2$CO$_2$H / Cu(100)

β = 0.05 - 1.0 K/s
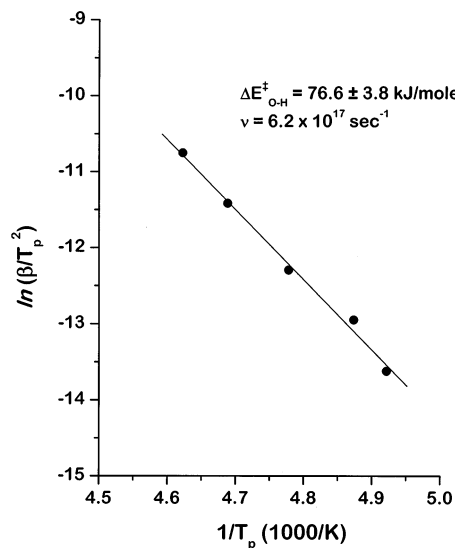
Figure 9. Plot of $\ln(\beta/T_p^2)$ versus $1/T_p$ for CF$_3$CF$_2$HCO$_2$H deprotonation on the Cu(100) surface measured heating rates varying from β = 0.05 to 1 K/s. The slope yields a value of $\Delta E^{\ddagger}_{O-H}$ = 76.6 kJ/mol.

ζ vs. T - Acid Deprotonation / Cu(100)
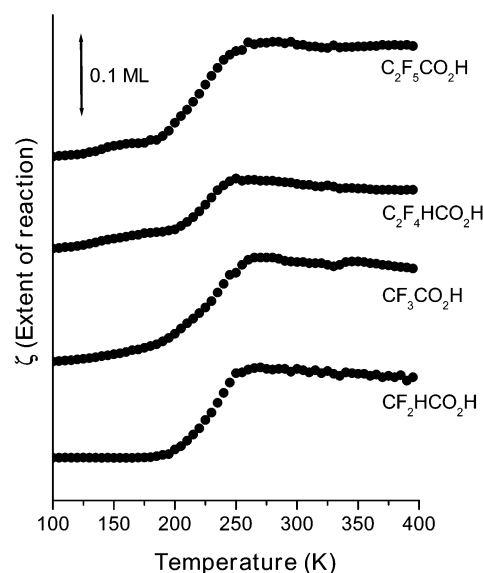
Figure 10. The extent of deprotonation (ζ) measured as the carboxylate coverage versus surface temperature for CF$_2$HCO$_2$H, CF$_3$CO$_2$H, C$_2$F$_2$HCF$_2$CO$_2$H, and CF$_3$CF$_2$CO$_2$H deprotonation on the Cu(100) surface at coverages of roughly 0.1 ML.

derivatives of the $\theta(T)$ curves give T_p for each of the acids. The values of $\Delta E^{\ddagger}_{O-H}$ were then calculated at various coverages using Redhead's equation and the value of $\nu = 6.2 \times 10^{17}$ s^{-1} obtained for CF$_2$HCF$_2$CO$_2$H. The values of $\Delta E^{\ddagger}_{O-H}$ versus initial acid coverage are shown in Figure 11 for all fours acids. In all cases, the $\Delta E^{\ddagger}_{O-H}$ increases with increasing coverage but then plateaus as the coverage increases past 0.25 ML. More importantly from the perspective of this work there is a consistent decrease in the $\Delta E^{\ddagger}_{O-H}$ as the degree of fluorination of the acid is increased.

Carboxylic Acid Deprotonation on Cu(100)

J. Phys. Chem. B, Vol. 108, No. 11, 2004 **3509**

$\Delta E^{\ddagger}_{O-H}$ vs. Coverage - Acids / Cu(100)
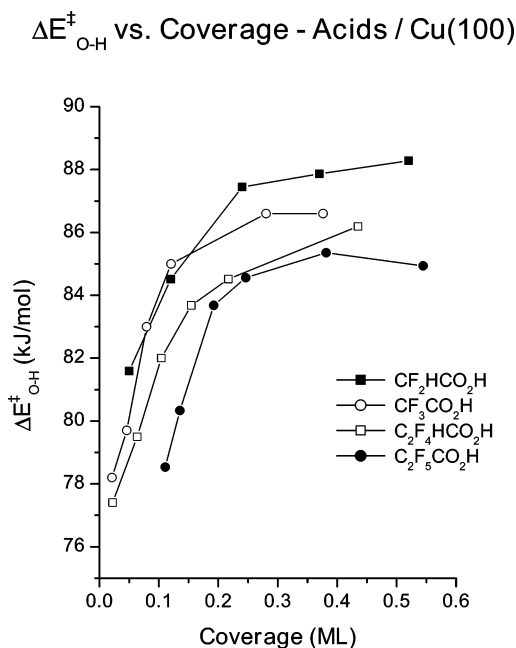
Figure 11. $\Delta E^{\ddagger}_{O-H}$ versus initial acid coverage for CF$_2$HCO$_2$H, CF$_3$-CO$_2$H, C$_2$F$_2$HCF$_2$CO$_2$H, and CF$_3$CF$_2$CO$_2$H on the Cu(100) surface.

4. Discussion

4.1. Transition State for Acid Deprotonation on Cu (100). The goal of this work is to correlate the barriers to deprotonation, $\Delta E^{\ddagger}_{O-H}$, with the substituent constants, σ_F, for each of the acids in order to probe the nature of the transition state for acid deprotonation on the Cu(100) surface. To do this, however, we must first examine the dependence of $\Delta E^{\ddagger}_{O-H}$ on the acid coverage. Figure 11 shows the values of $\Delta E^{\ddagger}_{O-H}$ as a function of the acid coverage. At low coverages, the values of $\Delta E^{\ddagger}_{O-H}$ increase with coverage but then reach a constant value for each acid as the coverage is increased to $\theta > 0.25$ monolayers. Such a coverage-dependent $\Delta E^{\ddagger}_{O-H}$ has been observed by Lee et al. in a study of the deprotonation of acetic acid on the Cu(110) surface.[11] In that work, $\Delta E^{\ddagger}_{O-H}$ varied from 37.6 kJ/mol at low coverage to 106 kJ/mol at high coverage. The origin of the coverage dependence of $\Delta E^{\ddagger}_{O-H}$ is not clear but may arise from hydrogen bonding between adsorbed acid molecules. In the gas phase, acetic acid molecules form hydrogen-bonded dimers at high pressure. On the Pt(111) surface, Gao et al. found that acetic acid adsorbed at intermediate coverages will also form intermolecular hydrogen bonds.[18] The heat of acetic acid dimerization on the Pt(111) surface was reported to be ∼30.5 kJ/mol. Hydrogen bonding can increase the $\Delta E^{\ddagger}_{O-H}$ by stabilizing the acid in its protonated form on the surface. The coverage dependence of $\Delta E^{\ddagger}_{O-H}$ that we have observed on the Cu(100) surface is not as great as on the Cu(110) surfaces. The high coverage value of $\Delta E^{\ddagger}_{O-H} \approx 85-90$ kJ/mol for the fluorinated acids on the Cu(100) surface, however, is similar to the value of $\Delta E^{\ddagger}_{O-H} = 106$ kJ/mol observed on the Cu(110) surface. Furthermore, as will be shown below, one expects the value of $\Delta E^{\ddagger}_{O-H}$ to be lower for the fluorinated acids than for acetic acid.

Having determined the values of $\Delta E^{\ddagger}_{O-H}$ for all four acids at various coverages, correlations between the $\Delta E^{\ddagger}_{O-H}$ and the field substituent parameter, σ_F, can be examined. Since the activation energies are coverage dependent, we have made the correlations using the values in the limit of zero coverage, $(\Delta E^{\ddagger}_{O-H})_0$, and at a coverage of 1/2 ML, $(\Delta E^{\ddagger}_{O-H})_{1/2}$. The

TABLE 1: The Field Substituent Constants of the Fluoroalkyl Groups of Carboxylic Acids

substituent	field constant (σ_F)
CF$_2$H−	0.29[a]
CF$_3$−	0.38[a]
CF$_2$HCF$_2$−	0.41[b]
CF$_3$CF$_2$−	0.44[a]

[a] Table 1 of ref 24. [b] Interpolation of σ_F for CF$_2$H and CF$_3$CF$_2$.

LFER - Acid Deprotonation on Cu(100)
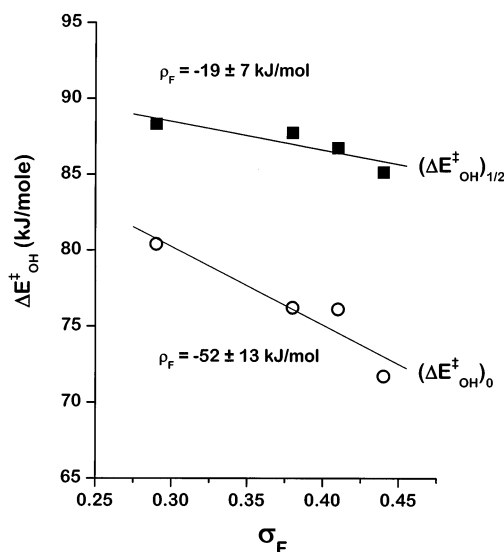
Figure 12. Linear free energy relationship for the carboxylic acid deprotonation reaction on the Cu(100) surface. The reaction constants are $\rho_F = -52 \pm 13$ kJ/mol in the limit of zero coverage and $\rho_F = -19 \pm 7$ kJ/mol at 1/2 ML coverage.

activation energies at zero and half coverages were determined from Figure 11. The values of $(\Delta E^{\ddagger}_{O-H})_0$ were estimated by extrapolating the region of the curve in which the $\Delta E^{\ddagger}_{O-H}$ still increases with coverage to the intercept with y-axis. The values of $(\Delta E^{\ddagger}_{O-H})_{1/2}$ were determined from the values of $\Delta E^{\ddagger}_{O-H}$ at coverages greater than 0.25 monolayers at which point they are coverage independent. The correlations between the $\Delta E^{\ddagger}_{O-H}$ and the σ_F take the form of linear free energy relationships.[23,24] The field substituent constants are empirical measures of the dipole moment of the substituent group. As shown in Table 1, increasing the fluorine content of the alkyl groups results in larger substituent constants. Note that the value of σ_F for the CF$_2$HCF$_2$− group has not been reported in the literature and has been estimated in this work by interpolating between the values for the CF$_3$ ($\sigma_F = 0.38$) and C$_2$F$_5$ ($\sigma_F = 0.44$) groups.[24] The correlations between the values of $\Delta E^{\ddagger}_{O-H}$ and σ_F yield straight lines as shown in Figure 12.

The nature of the transition state for acid deprotonation on the Cu(100) surface can be inferred from the slope of the LFER, ρ_F, also known as the reaction constant. For an elementary reaction with a transition state which is cationic with respect to the reactant, substituents with higher values of σ_F raise the activation barrier by destabilizing the cationic transition state with respect to the reactant. As an example, the β-hydride elimination reaction of alkoxides to aldehydes on the Cu(111) surface yields $\rho_F = 150$ kJ/mol.[2,3] Therefore, the transition state for β-hydride elimination is cationic, $[R-C^{\delta+}\cdots H^{\delta-}]^{\ddagger}$. If $\rho_F \approx 0$, then the electron density distribution in the transition state is not much different from that in the adsorbed reactant. This is

the case for dehalogenation reactions on the Ag(111) and Pd-(111) surfaces.[4-6] Finally, a negative value of ρ_F indicates that fluorination of the substituents stabilizes the transition state with respect to the adsorbed reactant. This implies that the transition state is anionic, as one would expect for the deprotonation of acids in the gas phase.

The LFER for deprotonation of the carboxylic acids shows that fluorination of the substituents on the acids lowers the value of the $\Delta E_{O-H}^{\ddagger}$, as illustrated in Figure 12. The values of ρ_F determined in the limit of low coverage and for a coverage of 1/2 ML are found to be $(\Delta E_{O-H}^{\ddagger})_0 = -52 \pm 13$ kJ/mol and $(\Delta E_{O-H}^{\ddagger})_{1/2} = -19 \pm 7$ kJ/mol, respectively. To put these values into perspective they can be compared with the values of the reaction constants for acid deprotonation and dehydrogenation in the gas phase. In the gas phase, the heat of deprotonation of CF_3CO_2H is 105 kJ/mol lower than that of CH_3CO_2H. The CF_3 group stabilizes the anionic acetate product, RCO_2^-.[25-27] The value of the reaction constant for carboxylic acid deprotonation in the gas phase can be estimated at $\rho_F = -104$ kJ/mol from the gas-phase acidities of acetic acid and its fluorinated derivatives.[23] In comparison, the reaction constant for simple, homolytic O–H bond cleavage of the carboxylic acids in the gas phase is $\rho_F = 0$ kJ/mol. In other words, fluorination of the methyl group in acetic acid does not have any influence on the relative energies of the gas-phase acids and their corresponding carboxyl radicals, $R-CO_2\bullet$. The range of values that we have found for the reaction constants for acid deprotonation on the Cu(100) are significant in magnitude to those for gas-phase acid deprotonation. This suggests that the transition state for acid deprotonation on the Cu(100) surface is anionic with respect to the reactant.

$$RCO_2H_{(ad)} \leftrightarrow [RCO_2^{\delta-}\cdots H^{\delta+}]^{\ddagger}$$

The reaction constant for acid deprotonation on the Cu(100) surface, $\rho_F = -19$ to -52 kJ/mol, is lower than that for deprotonation in the gas phase, $\rho_F = -104$ kJ/mol. One obvious explanation is that the charge separation in the transition state on the Cu(100) surface is not as large as that of the acetate anion and proton produced by gas-phase deprotonation. This is not surprising since the metal is likely to delocalize some of the charge on the carboxylate anion product adsorbed on the surface. Alternately, the presence of the metal may serve to screen the charged transition state in much the same way as water screens and stabilizes the carboxylate anions produced by acid deprotonation in the aqueous phase. The charge separation in the transition state is, however, consistent with the view based on the work function and XPS results that the product carboxylate on the Cu(100) surface should be considered anionic.

All four fluorinated acids studied in this work deprotonate spontaneously on the Cu(100) surface at temperatures in the range 150–300 K. The values of $\Delta E_{O-H}^{\ddagger}$ measured at high coverages of the fluorinated acids on Cu(100) fall in the range $\Delta E_{O-H}^{\ddagger} = 85-90$ kJ/mol and are similar to the value of $\Delta E_{O-H}^{\ddagger} = 106$ kJ/mol reported by Lee et al. for acetic acid on Cu(110).[11] Our linear free energy relationship depicted in Figure 12 predicts a value of $\Delta E_{O-H}^{\ddagger} = 94$ kJ/mol for acetic acid on the Cu(100) surface at high coverage. The principal difference between the results on the Cu(100) and Cu(110) surfaces is that the low coverage values of $\Delta E_{O-H}^{\ddagger}$ differ substantially. On the Cu(110) surface the value of $\Delta E_{O-H}^{\ddagger}$ for acetic acid is very coverage dependent and drops from $\Delta E_{O-H}^{\ddagger} = 106$ kJ/mol to $\Delta E_{O-H}^{\ddagger} = 37.6$ kJ/mol at low coverage. The coverage depen-

dence is attributed to stabilization of the initial state acid by hydrogen bonding as one increases the coverage. The difference between the Cu(100) and Cu(110) surface might be that the corrugated nature of the Cu(110) surface inhibits hydrogen bonding between adsorbed acids at low coverages, whereas this occurs quite readily at low coverages on the Cu(100) surface. The similarities between the results at high coverages on the two surfaces are satisfying; however, the differences at low coverages have yet to be resolved.

4.2. Thermochemistry of Acid Deprotonation on Cu(100). The fact that both the transition state and the carboxylate product of acid deprotonation on the Cu(100) surface are anionic with respect to the adsorbed acid does not imply that the transition state must be product-like. Hammond's postulate suggests that for an exothermic reaction the transition state occurs early in the reaction coordinate.[28] Although there is not enough data to determine the reaction energetics for deprotonation of the fluorinated acids used in this work on the Cu(100) surface, a Born–Haber cycle for deprotonation of acetic acid on the Cu(110) surface can be constructed. This is shown below and indicates that the acid deprotonation reaction is exothermic. The

$$\Delta E_{O-H} = -47 \text{ kJ/mol}$$
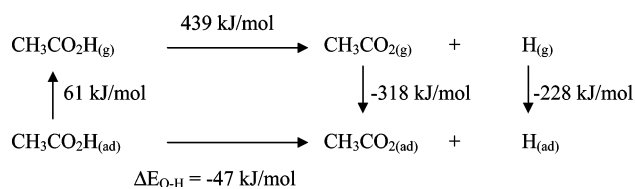
desorption energy of the acid is determined from Redhead's equation using the desorption temperature of 240 K reported by Bowker et al.[16] and a preexponential factor of 10^{13} s^{-1}. The heat of the homolytic acetic acid dehydrogenation reaction to acetyl and a hydrogen atom in the gas phase has been determined experimentally.[26,27] The adsorption energies of $\Delta E_{ads} = -318$ kJ/mol for acetyl and $\Delta E_{ads} = -228$ kJ/mol for a hydrogen atom on Cu(110) have been obtained from electronic structure calculations.[29,30] Other, experimentally and computationally determined values for these quantities suggest that they are even greater in magnitude and would make the energetics of the surface deprotonation reaction even more exothermic.[21,29] The Born–Haber cycle predicts the net reaction energy for acetic acid deprotonation on the Cu(110) surface to be $\Delta E_{O-H} = -47$ kJ/mol. In other words, the reaction is exothermic and according to Hammond's postulate would be reactant-like, occurring early in the reaction coordinate. To relate this analysis of the deprotonation energetics of acetic acid on the Cu(110) surface to those of the fluorinated acids on the Cu(100) surface we must consider the effects of fluorination on each of the relevant elementary steps of the Born–Haber cycle. Fluorination of ethanol has been shown to lower the desorption energy from the Ag(110) and Cu(111) surfaces slightly but not sufficiently to change the sign of the net energetics for the surface deprotonation reaction.[2,31] Similarly, fluorination of acetic acid has been shown to have very little influence on the energetics of homolytic O–H bond cleavage in the gas phase.[26,27] On the other hand, if the product carboxylates are anionic on the Cu surfaces, then fluorination ought to stabilize the product significantly with respect to the reactant and render deprotonation of the fluorinated acids even more exothermic than for acetic acid. This is analogous to the fact that fluorination of the acetic acids reduces the gas-phase heat of deprotonation substantially.[25-27] Thus all indications are that carboxylic acid deprotonation on the Cu(100) surface is exothermic and suggests, in accordance with Hammond's postulate and our
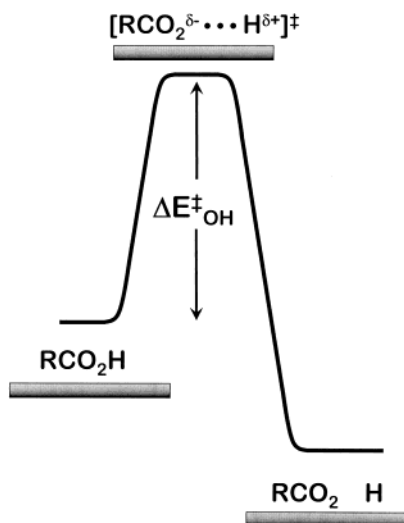
Figure 13. Potential energy diagram for acid deprotonation on the Cu(100) surface. The transition state is anionic with respect to the acid, and the reaction is exothermic.

experimental results, that the transition state is anionic and occurs early in the reaction coordinate. Figure 13 depicts a potential energy diagram for acid deprotonation that is consistent with our understanding based on the work presented in this paper.

Conclusion

CF$_2$HCO$_2$H, CF$_3$CO$_2$H, CF$_2$HCF$_2$CO$_2$H, and CF$_3$CF$_2$CO$_2$H all deprotonate on the Cu(100) surface at surface temperatures below 300 K. The field reaction constants for the acid deprotonation reaction derived from LFERs are $\rho_F = -52 \pm 13$ kJ/mol in the limit of zero coverage and $\rho_F = -19 \pm 7$ kJ/mol at 1/2 ML coverage. This indicates that the transition state for acid deprotonation on the Cu(100) surface is anionic with respect to the reactant.

References and Notes

(1) Gellman, A. J. *Acc. Chem. Res.* **2000**, *33*, 19−26.
(2) Dai, Q.; Gellman, A. J. *J. Phys. Chem.* **1993**, *97*, 10783−10789.
(3) Gellman, A. J.; Dai, Q. *J. Am. Chem. Soc.* **1993**, *115*, 714−722.
(4) Buelow, M. T.; Zhou, G.; Gellman, A. J.; Immaraporn, B. *Catal. Lett.* **1999**, *59*, 9−13.
(5) Buelow, M. T.; Immaraporn, B.; Gellman, A. J. *J. Catal.* **2001**, *203*, 41−50.
(6) Buelow, M. T.; Gellman, A. J. *J. Am. Chem. Soc.* **2001**, *123*, 1440−1448.
(7) Gulkova, D.; Kraus, M. *J. Mol. Catal.* **1994**, *87*, 47−55.
(8) Gulkova, D.; Kraus, M. *Collect. Czech. Chem. Commun.* **1992**, *57*, 2215−2226.
(9) Kraus, M. *Adv. Catal.* **1980**, *29*, 151−196.
(10) Parker, B.; Immaraporn, B.; Gellman, A. J. *Langmuir* **2001**, *17*, 6638−6646.
(11) Lee, J. G.; Ahner, J.; Mocuta, D.; Denev, S.; Yates, J. T. *J. Chem. Phys.* **2000**, *112*, 3351−3357.
(12) Caputi, L. S.; Chiarello, G.; Lancellotti, M. G.; Rizzi, G. A.; Sambi, M.; Granozzi, G. *Surf. Sci.* **1993**, *291*, L756−L758.
(13) Bowker, M.; Rowbotham, E.; Leibsle, F. M.; Haq, S. *Surf. Sci.* **1996**, *349*, 97−110.
(14) Crapper, M. D.; Riley, C. E.; Woodruff, D. P. *Surf. Sci.* **1987**, *184*, 121−136.
(15) Hayden, B. E.; Prince, K.; Woodruff, D. P.; Bradshaw, A. M. *Surf. Sci.* **1983**, *133*, 589−604.
(16) Bowker, M.; Madix, R. J. *Appl. Surf. Sci.* **1981**, *8*, 299−317.
(17) Ying, D. H. S.; Madix, R. J. *J. Catal.* **1980**, *61*, 48−56.
(18) Gao, Q. Y.; Hemminger, J. C. *Surf. Sci.* **1991**, *248*, 45−56.
(19) Avery, N. R. *J. Vac. Sci. Technol.* **1982**, *20*, 592−593.
(20) Wagner, C. D.; Riggs, W. M.; Davis, L. E.; Moulder, J. F.; Muilenberg, G. E. *Handbook of X-ray Photoelectron Spectroscopy*; Perkin-Elmer Corp.: Eden Prairie, MN, 1979.
(21) Kolovos-Vellianitis, D.; Kammler, T.; Kuppers, J. *Surf. Sci.* **2000**, *454*, 316−319.
(22) Redhead, P. A. *Vacuum* **1962**, *12*, 203−211.
(23) Taft, R. W. *Prog. Phys. Org. Chem.* **1983**, *14*, 247−350.
(24) Hansch, C.; Leo, A.; Taft, R. W. *Chem. Rev.* **1991**, *91*, 165−195.
(25) Caldwell, G.; Renneboog, R.; Kebarle, P. *Can. J. Chem.-Rev. Can. Chim.* **1989**, *67*, 611−618.
(26) Lias, S. G.; Bartmess, J. E.; Liebman, J. F.; Holmes, J. L.; Levin, R. D.; Mallard, W. G. *J. Phys. Chem. Ref. Data* **1988**, *17*, 1.
(27) Cumming, J. B.; Kebarle, P. *Can. J. Chem.-Rev. Can. Chim.* **1978**, *56*, 1−9.
(28) Hammond, G. S. *J. Am. Chem. Soc.* **1955**, *77*, 334−338.
(29) Karis, O.; Hasselstrom, J.; Wassdahl, N.; Weinelt, M.; Nilsson, A.; Nyberg, M.; Pettersson, L. G. M.; Stohr, J.; Samant, M. G. *J. Chem. Phys.* **2000**, *112*, 8146−8155.
(30) Bae, C. S.; Freeman, D. L.; Doll, J. D.; Kresse, G.; Hafner, J. *J. Chem. Phys.* **2000**, *113*, 6926−6932.
(31) Dai, Q.; Gellman, A. J. *J. Phys. Chem.* **1991**, *95*, 9443−9448.